Energy xxx (2015) 1–9

Contents lists available at ScienceDirect

Energy

journal homepage: www.elsevier.com/locate/energy

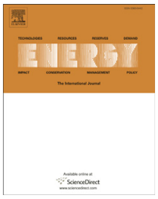

Benefits of weakening in thermogravimetric signals of hemicellulose and lignin for producing briquettes from soybean crop residue

Sandip Gangil*

Agricultural Energy and Power Division, Central Institute of Agricultural Engineering, Bhopal 462038, Madhya Pradesh, India

ARTICLE INFO

Article history:
Received 28 December 2013
Received in revised form
22 December 2014
Accepted 6 January 2015
Available online xxx

Keywords:
Kinetics
Thermogravimetry
Activation energy
Briquetted biofuel
Soybean crop residues

ABSTRACT

Thermogravimetric signals of hemicellulose and lignin were found to subside due to the binderless briquetting of soybean crop residue. Minor but distinct thermogravimetric signals of secondary charring reactions were observed in raw crop residue and its briquetted biofuel. The bio-component related kinetics was evaluated using the Kissinger method. Activation energy level of intrinsic cellulosic biopolymer was found higher in briquette than that level in crop residue. The activation energy profile with respect to conversion fraction for raw residue and its briquette was analyzed by the Kissinger–Akahira–Sunose method. The activation energy profile of briquette was superior to raw residue of soybean crop showing the better thermal stability in briquetted biofuel, highlighting the benefits of briquetting process. In addition to the physico-chemical transformations occurred in lignin, the hemicellulose and cellulose related transitions were also expected to play positive role for briquetting.

© 2015 Elsevier Ltd. All rights reserved.

1. Introduction

Briquette is the compact solid fuel made from the loose crop residues [1–5]. The formation of briquettes is positive toward better utilization of loose CR (crop residues) for energy generation [4–7]. The briquettes are used as an alternate to wood in combustion and gasification devices. The crop residues are available in a huge quantity after the harvest of the crop [8,9] which can be utilized as a substantial and sustainable renewable energy source. The major constraint in utilization of crop residues as energy source is their low bulk densities [2,4,5,9–11] which vary from 100 to 200 kg/m^3. The low bulk density poses problems in handling, transportation and storage of crop residues. Due to less density, the energy density of crop residues is low and the CR also requires a lot of space for the transportation. The biomass based energy generation systems need the biofuel with better flow ability. The fuel having uniform size and shape has better flow ability. Better flow ability of fuel in bio-reactors reduces the chocking and blockage in the bio-energy systems. The easy flow property of crop residues in the bio-energy reactors is poor due to their light weight and irregular shape and size. To deal with these constrains, it is better to convert the crop residues into high density uniform solid biofuel, i.e. briquettes. Briquetting [1–7,9–20] is the process to compress the crop residues to make uniformly sized compact solid pieces of high density, which can be effectively used as fuel. Briquettes can be produced from the loose biomass until the density of 1200 kg/m^3. These can cleanly be burnt and therefore are eco-friendly. In India, briquettes are mostly manufactured from saw dust, bagasse, mustard stalk, groundnut shell, cotton stalk and pigeon pea stalks, etc. Basically, almost all lignocellulosic crop residues can be briquetted by using the optimum process parameters of the briquetting [2–7,10]. Mainly, three types of commercial briquetting systems are in use for generation of briquettes which are; i) Screw-press type, ii) Piston-press (die-punch) type and iii) Rotary dies and roller type [1–7,9–20].

In piston-press type systems, a die exists. The raw bio-material is pressed by the piston (ram) through a die, putting very heavy pressure on bio-materials. The raw biomaterial is heated due to high pressure, and its temperature goes up. The inner biomatrix changes and a compact briquette comes out of the system. In screw press type briquetting machine, a conveyer screw conveys the raw material to the die. The conveyer screw is designed in a manner to exert heavy pressure to raw bio-material when the bio-material reaches to the die. The die in the screw press type systems are basically an opening to allow the densified extruded briquettes, out of the machine. A difference in the piston-press and screw-press type briquetting machines is that the first exert pressure in

---

* Tel.: +91 755 2521132, +91 9754913685; fax: +91 755 2734016.
E-mail addresses: gangilsandip@yahoo.co.in, gangils@yahoo.com, gangil@ciae.res.in.

http://dx.doi.org/10.1016/j.energy.2015.01.018
0360-5442/© 2015 Elsevier Ltd. All rights reserved.

Please cite this article in press as: Gangil S, Benefits of weakening in thermogravimetric signals of hemicellulose and lignin for producing briquettes from soybean crop residue, Energy (2015), http://dx.doi.org/10.1016/j.energy.2015.01.018

regular pulses, whereas in second the pressure is exerted continuously. At present, both types of system are in use to briquette the bio-materials. The energy consumption per unit output is less in piston-press briquetting system [2–5,10].

Briquetting process can be done using the binder or without binder. Binderless briquetting process demands high pressure as well as high temperature as compared to the briquetting with binder. The binders are materials that facilitate the binding of the bio-particles when subjected to relatively low pressure and temperature. The need of binder depends on the bio-material being briquetted. The use of binders increases the production cost of briquettes. Binder may also hinder in the burning process of briquettes. Almost all lignocellulosic material can be briquetted without binder. Cellulose, hemicellulose, lignin are the main components of CR. In briquetting, the raw CR is compressed at high pressures, and temperatures exceeding 200–250 °C are expected in die-region to relax and melt the lignin which fuses the CR particles into briquettes of designed shape and size [2,10]. Lignin works like a binding agent. This is basically a change in the inner bio-matrix due to high pressure and temperature exerted on the bio-material during the briquetting. This can be studied using the TGA (thermogravimetric analysis) wherein a bio-material is subjected to heat in precisely monitored chamber. The thermal degradation of different constituents of bio-material can be identified using TGA for a specific bio-material. Thermal degradation of bio-materials can be assumed to happen in the stages of moisture release, hemicellulose degradation, cellulose degradation and lignin degradation as stated by Vasile et al. [21]. Caballero et al. [22] explained the thermal degradation of lignocellulosic bio-materials as the summation of the independent degradations of their main components. López-González et al. [23] also stated that the devolatilization curve of bio-materials could be taken as the sum of the corresponding individual components contributions. Leadakowicz and Stolarek [24] mentioned that the evolution of each volatile could be considered as a single first order reaction assuming that the constituents of bio-material were evolved by independent parallel reactions. According to Sanchez-Silva et al. [25] hemicellulose had a random and amorphous structure with low strength whereas cellulose had a strong crystalline structure. They also mentioned that lignin showed the highest thermal stability, decomposing in the broader temperature range (200–700 °C), studied and the DTG (differential thermogram) profile of lignin segment was the flattest [25]. Thermal degradation of lignin was very complex as it was heavily cross-linked highly-branched intrinsic biopolymer.

Using thermogravimetric data, the raw SCR (soybean crop residue) and its briquetted biofuel (SB) were compared to investigate about thermal stability of various specific bioconstituents. During briquetting, the crop residues undergoes through stresses due to high temperature and pressure in a semi-confined environment making internal changes in different components of bio-material. There are various methods for determination of kinetics [4,5,21–40] of thermal degradation, like Friedman method, Coats–Redfern method, Kissinger, Kissinger–Akahira–Sunose (KAS) method, and Ozawa–Flynn–wall (OFW), etc. The KAS, OFW and Coats–Redfern methods are integral isoconversional methods whereas Friedman is differential method [4,5,26,27,29]. Kissinger method is basically not an isoconversional method. This method is used to find the kinetics of different biocomponents based of the temperature-location corresponding to maximum degradation rate associated with a specific bioconstituent. In Kissinger method also, studies at the different β are required to find the activation energies related to different components of the biomaterials. At the other end, Kissinger–Akahira–Sunose (KAS) method has ability to scan the kinetics in relation to conversion fraction of mass during thermal degradation. Kinetics is needed for designing of the energy devices to use the raw biomaterials and their briquettes as biofuel. This article presents comparative thermogravimetric kinetics of soybean crop residue and its briquette. Thermogravimetric changes occurring due to briquetting stresses in the biomaterial were explained on the basis of activation energy profiles of SCR and SB.

2. Materials and methods

The residues of soybean crop were taken for study. Thermogravimetric analyses of crushed biomaterial of SCR and crushed biomaterial of the briquettes (made from SCR) were done to understand the internal physico-chemical transformations, affecting the thermal stability of the different biocomponents, occurred during the briquetting process. Thermogravimetric analyzer (Model: pyris-6; Make: Perkin Elmer) was used. Thermogravimetry provided the information about the weight loss (%) of biomaterial with respect to the temperature or time (thermogram) during the thermal degradation process. The first order derivative (degradation rate profile) plot of the thermogram gave the weight loss rate *versus* temperature or time, i.e., about the degradation rate, %/min. Degradation rate profile is termed as “DTG (differential thermogram)”.

For analysis, the exactly same thermogravimetric heating method was taken for both types of materials. The heating method was to maintain the TGA temperature at 35 °C for two minutes and then to raise the temperature at different heating rates (β) from 35 °C to 1000 °C in the nitrogen (flow rate 30 ml/min) environment. Four β (10, 20, 30 and 40 °C/min) were used for TGA experiments. For TG-analysis, raw SCR were crushed and then crushed material was briquetted. The briquettes were again crushed for TG analysis. The sieve analysis was done for crushed raw SCR and crushed SB. The particle distributions of crushed biomaterials from both (i.e., SB and SCR) were done in the size ranges of >0.2 mm, 0.2–0.4 mm, 0.4–0.7 mm, 0.70–1.4 mm, 1.4–1.7 mm and <1.7 mm. The specimens for TG-experiments were taken from the size range (0.4–0.7 mm) which gave the highest portion of crushed material (38–40% of total crushed biomaterial) in sieve analysis. Therefore, the particle size selected for TG-experiment was 400–700 μm for biomaterials obtained by crushing the SB and SCR. Hence, for TG-analysis, the samples were drawn from the crushed form of the SCR and SB, having similar particle size and similar masses. The masses taken for repetitive TGA runs for SCR and SB were 10 ± 2 mg. The pyris-6 thermogravimetric analyzer used the exactly same crucibles for all runs. As the particle size for TG-samples taken from biomaterial of SB and SCR was same (400–700 μm), the effects of bulk density and porosity, especially during TG-experiments, were minimized. Therefore, the present paper essentially presents the changes occurring in the intrinsic biopolymeric components due to briquetting stresses.

The bulk densities of soybean crop residues, brought from the farmer's fields, were 120 ± 20 kg/m^3 (ar). The SCR was crushed and the bulk density of crushed SCR was 245 ± 5 kg/m^3. For forming the

Table 1
Characterization of crushed SCR and SB, used for TG-analysis.

	Proximate analysis % (db)			Ultimate analysis % (db)				Density (kg/m^3)
	Moisture	Volatiles	Ash	C	H	N	S	
Crushed SCR (400–700 μm)	9 ± 3	72 ± 3	4.0 ± 0.3	39	7	2	0.5	245 ± 5
Crushed SB (400–700 μm)	7 ± 3	70 ± 3	6.5 ± 0.3	40	6	2	0.5	250 ± 5

Please cite this article in press as: Gangil S, Benefits of weakening in thermogravimetric signals of hemicellulose and lignin for producing briquettes from soybean crop residue, Energy (2015), http://dx.doi.org/10.1016/j.energy.2015.01.018

briquettes, the crushed SCR was compacted using a commercially available piston-press type biomass briquetting machine (rated capacity 500 kg/h; rated power 35 kW). The machine is shown as supplementary information. Due to heavy pressure exerted on raw crushed SCR by briquetting machine, the temperature at the die of briquetting machine increased until 220 ± 20 °C. The bulk and true densities of formed briquettes were 650 ± 20 kg/m^3 and 1135 ± 15 kg/m^3, respectively. It showed the densification of the level of 3–4 times due to briquetting. The briquetted biofuels were again crushed (bulk density: 250 ± 5 kg/m^3) for TG-analysis. The characterization for the crushed SCR and crushed SB is given in Table 1, wherein the volatiles shown are excluding the moisture. The ash contents of SB were higher (about 2.5%) than the ash contents of SCR. This was true because the SCR underwent through briquetting stresses to form the SB. During the briquetting, the some portion of moisture (about 1–2%) and lighter volatiles (about 2–3%) were removed. As ash is expected to remain in the solid substances during the briquetting stresses, the values of ash contents was increased (about 2.5%) in SB.

3. Theory of thermal kinetics

The basic kinetics [26–30] of thermal degradation of biomass is defined as;

$$\frac{d\alpha}{dt} = k(T)f(\alpha) \tag{1}$$

where; α = conversion fraction, T = reaction temperature (absolute), t = reaction time, k(T) = chemical reaction kinetics Arrhenius constant, and f(α) = reaction model.

$$\alpha = \frac{(w_i - w_t)}{(w_i - w_\infty)} \tag{2}$$

where; the w_i, w_t and w_∞ are the masses of biomaterial at initial, instantaneous and final stages of decomposition, respectively.

$$k(T) = Ae^{\left(-\frac{E}{RT}\right)} \tag{3}$$

where; A = Arrhenius pre-exponential factor, R = Universal gas constant, E = activation energy.

$$f(\alpha) = (1-\alpha)^n \tag{4}$$

where; n = reaction order.

$$\text{Heating rate,} \quad \beta = \frac{dT}{dt} \tag{5}$$

By putting (3) in Equation (1), the Equation (1) can be written as;

$$\frac{d\alpha}{dt} = Ae^{\left(-\frac{E}{RT}\right)}f(\alpha) \tag{6}$$

By putting (5) in (6), the Equation (6) becomes;

$$\frac{d\alpha}{dT} = \frac{A}{\beta}e^{\left(-\frac{E}{RT}\right)}f(\alpha) \tag{7}$$

The Equation (6) can be written as;

$$\frac{d\alpha}{f(\alpha)} = \frac{A}{\beta}e^{\left(-\frac{E}{RT}\right)}dT \tag{8}$$

Integrating (7) on both side;

$$g(\alpha) = \int_{\alpha_i}^{\alpha_o} \frac{d\alpha}{f(\alpha)} = \frac{A}{\beta}\int_{T_i}^{T_o} e^{\left(\frac{-E}{RT}\right)} dT \tag{9}$$

where; T_i = reaction temperature at initiation, T_o = Temperature at the end, α_i = conversion fraction at initiation and α_o = conversion fraction at T_o.

Equation (9) does not have analytical solution and this can be written as [29];

$$g(\alpha) \equiv \frac{AE}{\beta R}\left[\frac{e^{(-x)}}{x} - \int_0^\infty \frac{e^{(-x)}}{x}dx\right] = \frac{AE}{\beta R}p(x) \tag{10}$$

where, x = E/RT which is reduced activation energy at temperature T, $p(x) = e^{-x}/x^2$

Based on (10), the Kissinger–Akahira–Sunose [26–30] method is arrived as Equation (11);

$$\ln\left(\frac{\beta}{T^2}\right) = \ln\left(\frac{AR}{E}\right) - \ln g(\alpha) - \frac{E}{RT} \tag{11}$$

The kinetics of thermal degradation of different components of a biomaterial can be found using Equation (11).

The kinetics can be evaluated in two ways. The first way is to do the isoconversional model treatment using KAS Equation (11). The second way is to do the kinetics computations using Kissinger method wherein kinetics related to different bioconstituents can be analyzed. In KAS method, isoconversional kinetics are determined assuming the terms ln g(α) and ln A as constant at a specific value of α in Equation (11). Thus, Equation (11) takes a form of linear equation with its slope equal to −E/R. The ln(β/T^2) *versus* 1/T plots were drawn for degradation at all heating rates for both the biomaterials. The isoconversional points were taken in complete conversion range (α = 0–1) at selected conversional fractions (α) of 0, 0.05, 0.10, 0.15, 0.20, 0.25, 0.30, 0.35, 0.40, 0.45, 0.50, 0.55, 0.60, 0.65, 0.70, 0.75, 0.80, 0.85, 0.90, 0.95 and 1.00. The KAS point (1/T, ln(β/T^2)) values at every selected α from each KAS curve related to all experimented β were extracted. The isoconversional lines (the linear plot of ln(β/T^2) *versus* 1/T) were drawn for each selected value of α. The activation energy was computed by finding the value of the slope from the isoconversional KAS kinetics lines drawn at different values of α.

The Kissinger method is given by Equation (12). In context to Kissinger method, Leadakowicz and Stolarek [24] stated that thermal degradation of a biomaterial can be assumed to occur as a sum of degradation of different constituents and the each component was assumed to degrade as single first order parallel reaction. The temperature (T_{max}), at which thermal degradation rate maximizes, is used in Kissinger analysis. Thermal degradation rate is basically the rate of conversion (dα/dt). The various peaks present in the differential thermogram of a bio-material are evaluated to obtain the T_{max}. At the highest point of each peak, the derivative of dα/dt approaches to zero. This method is standardized in USA (ASTME 1641-98 and ASTME 698-79) [24]. The T_{max} for the each lumps or peaks can be obtained at different β and the plot between ln(β/T^2_{max}) *versus* 1/T_{max} can be drawn to obtain the kinetics parameters using the Kissinger Equation (12) as described below [24,26,27,29,30];

$$\ln\left(\frac{\beta}{T^2_{max}}\right) = \ln\left(\frac{AR}{E}\right) - \frac{E}{RT_{max}} \tag{12}$$

Please cite this article in press as: Gangil S, Benefits of weakening in thermogravimetric signals of hemicellulose and lignin for producing briquettes from soybean crop residue, Energy (2015), http://dx.doi.org/10.1016/j.energy.2015.01.018

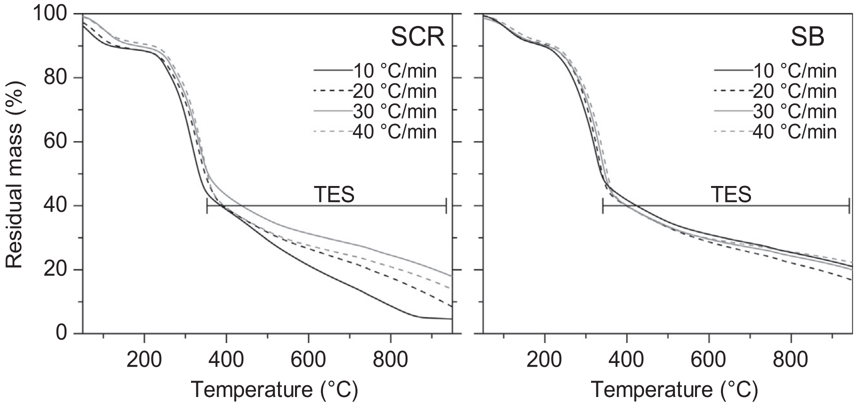

Fig. 1. Experimental mass loss curves (TG curves in % mass) for SCR and SB, showing lesser scattering of tail end segment, TES, (from 350 °C to end) in case of SB for same domain of experimented heating rates highlighting the biopolymeric consolidation due to briquetting stresses.

Basically, the Kissinger Equation (12) is specific form of the KAS Equation (11). However, the Kissinger method is not an isoconversional kinetics treatment, whereas KAS is an isoconversional treatment.

4. Results and discussion

Fig. 1 shows the experimental mass loss curve (TG curve showing residual % of mass) for SCR and SB. The dehydration segment in both cases could be seen till 180 °C. The dehydration ended around 180 °C and 160 °C in case of SB and SCR, respectively. The residual masses at the final stages of decomposition, w_∞, were higher in SB as compared to residual masses in SCR indicating higher residues in SB. The low scattering of tail end segment, TES, (from 350 °C to end) was clearly noticed in Fig. 1 showing the polymeric consolidation in SB. This was the similar finding as obtained by Gangil [5], for briquettes of pigeon pea stalks.

4.1. *Thermogravimetric signals of SCR and SB*

Thermal degradation rate profiles (DTG) of residue and its briquette are given in Fig. 2, whereas Fig. 3 shows the lignin and charring related zone of DTG. The variations of thermal degradation rate with respect to α for SCR and SB are given in Fig. 4. The changes occurring due to briquetting in the thermogravimetric signals of lignin degradation and charring reactions with respect to α are given in Fig. 5 for both bio-materials. To minimize the effects of bulk density and porosity, the same segment of particle size (400–700 μm) for crushed SCR and SB was used for TG-scans using the exactly same crucibles of pyris-6 thermogravimetric analyzer with sample weight 10 ± 2 mg. Thus, the variations, in the weight to volume ratio (bulk density), were minimum during TG-scans for both materials. As the particle size was in the same range, the porosity is also expected to vary minimally.

The region 50–180 °C was related with the dehydration or the release of the moisture in both types of biomaterials. The moisture peaks shifted to higher temperature region with increase in β in case of both, i.e., SCR and SB. On comparison of the moisture peaks, the locations of moisture related peak in SB were at higher temperatures than their corresponding locations in the SCR (Fig. 2). It indicated that during TG-degradation, the dehydration process continued until higher temperatures in case of SB than in case of SCR. Due to heating during the briquetting process, the moisture in outer portion of bioparticles of SCR escaped and the moisture, existing in the inner portions of bioparticles, remained in the SB. The conversion fraction periods (α-spans) associated with the dehydration was 0–0.12 and 0–0.10 for SCR and SB, respectively (Fig. 4). This signified that about 2% moisture difference was between the biomaterials from SCR and SB which was in agreement with the results mentioned in Table 1.

Hemicellulose [4,5,30–34] TG-signals were seen in the region of 180–300 °C in (Fig. 2) SCR and these signals were not distinctly visible in the SB. Highest peaks related to cellulose [4,5,21–25,30–39] were located in temperature range of 300–350 °C in both biomaterials. The hemicellulose degradation rates were lower than the rates during cellulosic degradation.

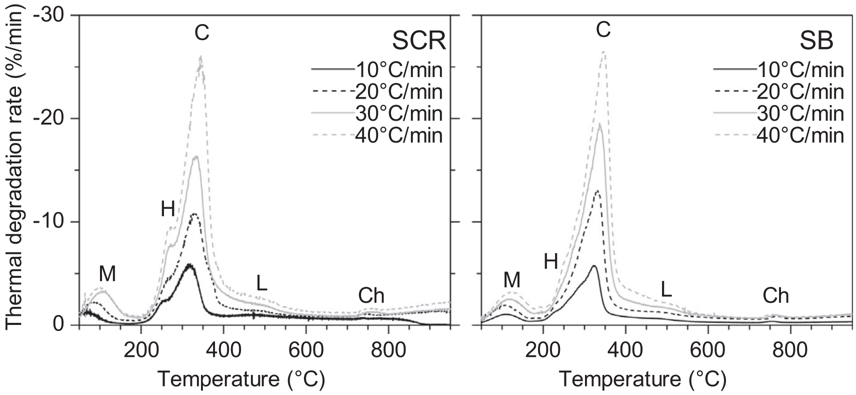

Fig. 2. Comparison of thermal degradation rate profiles of soybean crop residue (SCR) and its briquette (SB) (M-moisture, H-hemicellulose, C-cellulose, L-lignin and Ch-charring).

Please cite this article in press as: Gangil S, Benefits of weakening in thermogravimetric signals of hemicellulose and lignin for producing briquettes from soybean crop residue, Energy (2015), http://dx.doi.org/10.1016/j.energy.2015.01.018

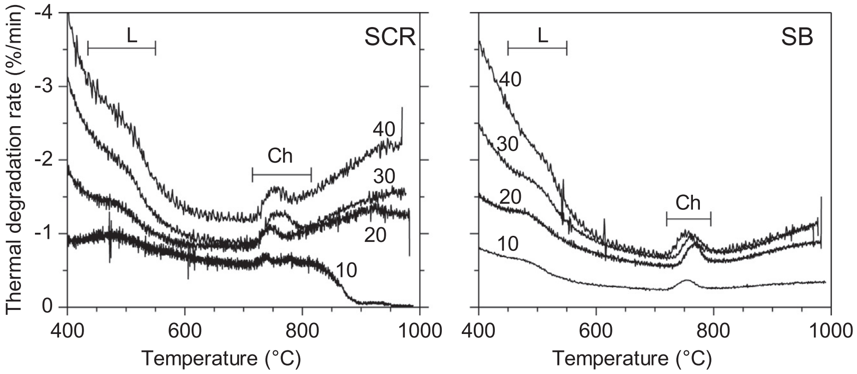

Fig. 3. Lignin and charring zone of thermal degradation rate profile of soybean crop residue (SCR) and its briquette (SB) (the number given close to each curve is the heating rates (°C/min) associated with that particular curve) (L-lignin and Ch-charring).

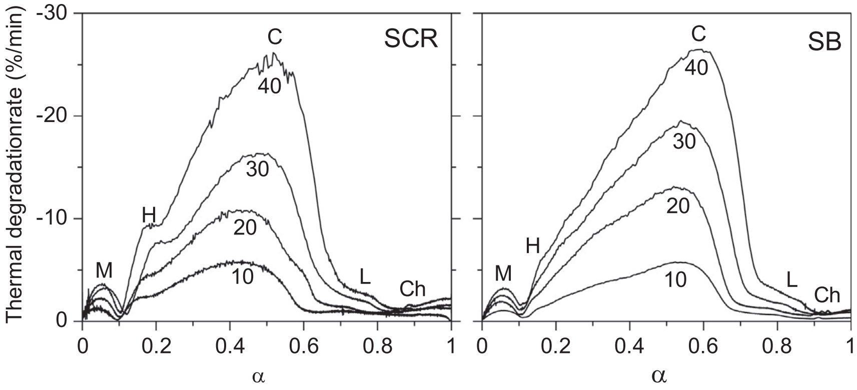

Fig. 4. Comparison of α-variance of thermal degradation rate for SCR and SB. (M-moisture, H-hemicellulose, C-cellulose, L-lignin and Ch-charring) (the number given close to each curve is the heating rates (°C/min) associated with that particular curve).

According to López-González et al. [23] during cellulose degradation, a complex set of reactions as denitration and deacetylation, scission of O—N, C—O, C—C and C—H bonds might take place. During hemicellulose degradation, the breakdown of C—O—C and some pyranose C—C bonds was expected [23]. Vasile et al. [21] indicated that hydrocarbons, aldehydes, ketones, acids, alcohols and others were generated by the primary pyrolysis of hemicelluloses and cellulose within the 290–400 °C region.

The lignin related thermogravimetric signatures [4,5,22–26,30,31,33,34,36,30,40] were observed near the temperature 500 °C (Fig. 3) in both biomaterials. The lignin degradation was expected to impact a three-dimensional structure consisting of phenylpropane coupled with C—C or C—O—C bonds whose activity covered a wide range of temperatures as suggested by López-González et al. [23]. The phenols and alcohols were the dominant volatiles released from lignin pyrolysis as stated by López-González et al. [23]. The shifting of different peaks towards the higher temperature was observed with the increase in β for cellulose and lignin. The lignin related degradation rate was always lower at each β in case of SB as compared to the SCR. Due to physico-chemical transformations in the biomaterial, occurred because of the briquetting stresses, it was expected that thermal stability might

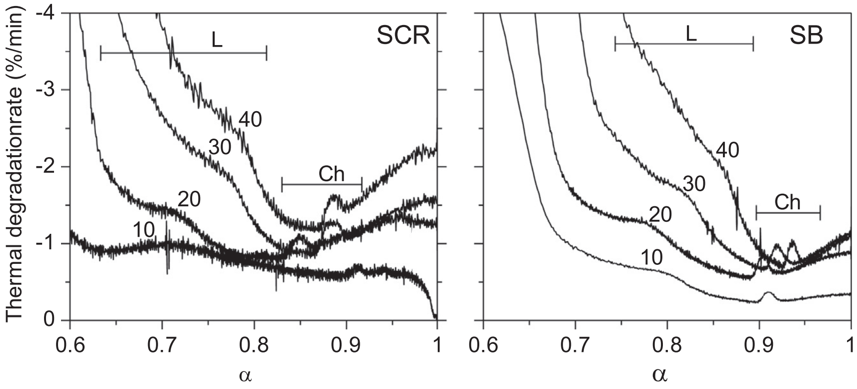

Fig. 5. Lignin and char zone of thermal degradation rate with respect to α-variance for SCR and SB at different heating rates (the number given close to each curve is the heating rates (°C/min) associated with that particular curve) (L-lignin and Ch-charring).

Please cite this article in press as: Gangil S, Benefits of weakening in thermogravimetric signals of hemicellulose and lignin for producing briquettes from soybean crop residue, Energy (2015), http://dx.doi.org/10.1016/j.energy.2015.01.018

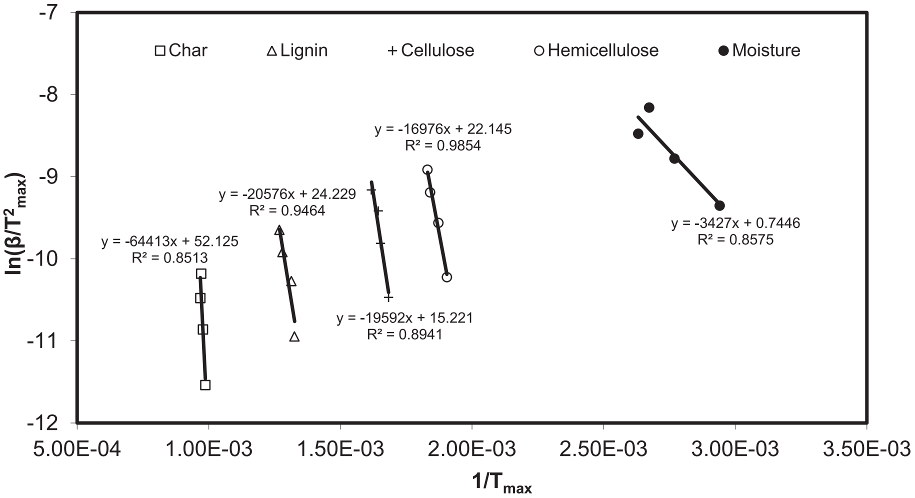

Fig. 6. Kissinger kinetic plot for different biocomponents of the SCR (where; y = $\ln(\beta/T^2_{max})$ and x = $1/T_{max}$).

enhance in SB which was explained using the activation energy analysis later in this writing. Gangil [4,5,30] stated that in case of stresses, either due to pressure or temperature or both, on the lignocellulosic biomaterials, the lignin in biomaterial first relaxed, then melted during stresses, and finally solidified in final-product (i.e., briquettes in present discussion). This article considered that the solidification of melted lignin was the one of the probable major causes of thermal stability in SB.

The peaks near the 750 °C in SCR and SB (Fig. 3) were ascribed to charring as secondary reactions occurring in thermal degradation of hemicellulose and lignin. In this region, complex reactions occurred at high temperature. This region was characterized by the evolution of hydrogen and methane in case of thermal degradation of lignocellulosic biomaterials due to charring. Idris et al. [40] experimented lignocellulosic biomaterial (palm kernel shell) and found charring TG-signals in the higher range of reaction temperature (700–750 °C), in their TG-experimentation under pyrolysis conditions. These signals were ascribed to release of methane or hydrogen by them. Gangil [4,5] stated that the region of 700–750 °C could be represented by release of methane (700–730 °C) and release of hydrogen (near 750 °C) due to charring reactions in case of pigeon pea stalk and its briquetted biofuel, respectively. Abdullah et al. [41] mentioned that the charring TG-signals might be due to the secondary reactions in lignin degradation. During the thermal decomposition of lignocellulosic materials (like wood), the volatiles, being produced as primary reactions, interfere with the carbonaceous residues, char. The hot char may cause the secondary reactions to occur in volatiles [42]. Beyler and Hirschler [42] stated that charring in woody material may be due to degradation of lignin. Author considered that the secondary charring reactions leading to evolution of methane or hydrogen or both may be during the later phase of thermal degradation of hemicellulose and lignin.

The degradation zones of SCR (Fig. 4) related to the moisture, hemicellulose, cellulose, lignin and charring are clearly depicted in α-range of 0–0.1, 0.15–0.25, 0.25–0.7, 0.65–0.80 and 0.80–0.95, respectively. At 20 °C/min, the thermogravimetric profile also indicated the existence of a lump at α-value of 0.6 which was also related with the cellulose. Cellulose may show more than one peaks during thermal degradation as indicated by Vasile et al. [21]. They mentioned that in the thermal decomposition of cellulose, the hydrolysis, oxidation and dehydration processes were side reactions and therefore, the step corresponding to the cellulose decomposition might be divided into two steps, depending on the

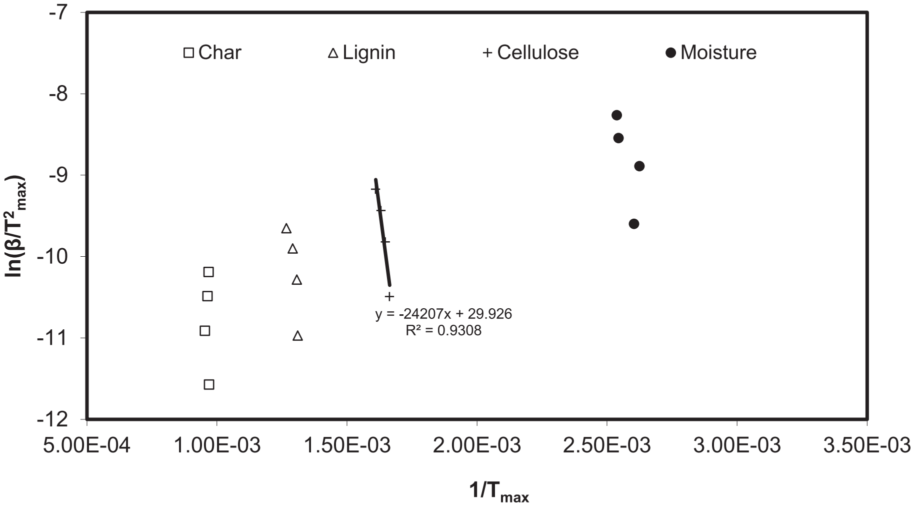

Fig. 7. Kissinger kinetic plot for different biocomponents of the SB. (where; y = $\ln(\beta/T^2_{max})$ and x = $1/T_{max}$).

Please cite this article in press as: Gangil S, Benefits of weakening in thermogravimetric signals of hemicellulose and lignin for producing briquettes from soybean crop residue, Energy (2015), http://dx.doi.org/10.1016/j.energy.2015.01.018

sample's nature [21]. According to them, cellulose followed two competitive reactions which were depolymerization of residual cellulose followed by the volatilization of levoglucosan [21]. Gangil [43] published the work on the splitting of cellulose related signals in cashew shell in which two cellulose related peaks were observed. The similar explanations were agreed in present study. In case of SB, the different zones related with the moisture, cellulose, lignin and charring were in the α-range of 0–0.12, 0.2–0.75, 0.75–0.90 and 0.9–0.95, respectively (Fig. 4). The hemicellulose presence was undistinguishable in SB, but minor lumps located at α-value of 0.15 at all heating rates were seen.

The charring signals were located at α-value of 0.91, 0.85, 0.88 and 0.89 at β of 10, 20, 30 and 40 °C/min, respectively, in case of SCR. In SB, these TG-signals were at α-value of 0.91, 0.90, 0.92 and 0.94 at β of 10, 20, 30 and 40 °C/min, respectively (Fig. 5). Minor peaks near the 780 °C in SCR can be seen in Fig. 3, at 10 °C/min, again associated with charring. In SCR, these peaks near 750 °C and 780 °C fell in the α-region of 0.8–0.9 and 0.9–0.95, respectively. In SB, only charring peaks near 750 °C were seen which reflected in α-region of 0.9–0.95 (Fig. 5). The degradation rates in charring zone were lower in SB than in SCR (except at β = 20 °C/min). The charring signals in the SB were sharper than these signals in SCR. In general, the locations of these TG-signals shifted towards lower temperature with increase in β in SCR. The presence of these TG-signals in SCR and SB was due to the charring during the secondary reactions related to hemicellulose and lignin degradation.

By comparing the α-zones related with SB and SCR, it was concluded that the hemicellulose and lignin signals weakened due to briquetting. The weak TG-signals of a specific biocomponent in particular biomaterial are indicator of thermal stability of that component in comparative studies. The thermogravimetric signals ascribed to the charring reactions shifted toward higher α-values in case of SB. The role of hemicellulose was positive for formation of briquettes [44].

4.2. Kissinger kinetics

All the temperatures (T_{max}) at the maximum value of dα/dt in the different regions (moisture, hemicellulose, cellulose, lignin and charring) were extracted for both the biomaterials at all four experimented heating rates. At these temperatures (T_{max}) the rate of change of dα/dt (change in the reaction rate ($d^2\alpha/dt^2$)) approaches to the zero indicating that the acceleration or retardation in conversion is nearly zero at T_{max} and the thermal degradation at T_{max} occurs at a constant dα/dt. Therefore, the non-accelerating constant thermal degradation reaction is expected at T_{max}.

Table 2
Kissinger kinetics of SCR and SB.

Peak number	Equation of linear fitting	R^2	Activation energy (kJ/mole)	Pre-exponential factor, A (min^{-1})
Soybean crop residue (SCR)				
Moisture	$y = -3427x + 0.7446$	0.86	28.5	−1.01E+03
Hemicellulose	$y = -16{,}976x + 22.145$	0.99	141.1	5.26E+04
Cellulose	$y = -20{,}576x + 24.229$	0.95	171.1	6.56E+04
Lignin	$y = -19{,}592x + 15.221$	0.89	162.9	5.33E+04
Char	$y = -64{,}413x + 52.125$	0.85	535.6	2.55E+05
Briquette (SB)				
Moisture	$y = -9861.8x + 16.598$	0.55	–	–
Hemicellulose	–	–	–	–
Cellulose	$y = -24{,}207x + 29.926$	0.93	201.3	8.23E+04
Lignin	$y = -25{,}068x + 22.243$	0.74	–	–
Char	$y = -6198.8x - 4.8151$	0.01	–	–

Where; $y = \ln(\beta/T^2_{max})$ and $x = 1/T_{max}$.

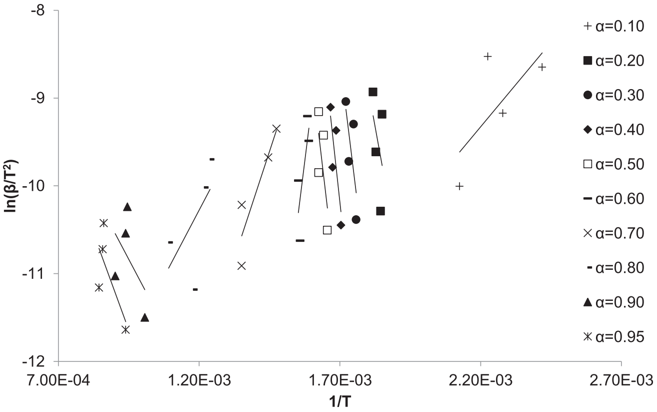

Fig. 8. KAS kinetic lines for SCR at different isoconversional fraction.

Kissinger kinetic lines, $\ln(\beta/T^2_{max})$ *versus* $1/T_{max}$, were plotted to obtain activation energy and pre-exponential factor pertaining to different bioconstituents of SCR and SB as given in Figs. 6 and 7, respectively. For SCR, the Kissinger points ($1/T_{max}$, $\ln(\beta/T^2_{max})$) could be obtained from TGA data for all the constituents namely moisture, hemicellulose, cellulose, lignin and charring segment. In case of SB, the points ($1/T_{max}$, $\ln(\beta/T^2_{max})$) could not be obtained for hemicellulose. Further, the activation energy for hemicellulose, lignin and charring segments was not computed for SB owing to poor correlation between the values of the $\ln(\beta/T^2_{max})$ and $1/T_{max}$. The kinetic parameters determined for different components of bio-materials are given in Table 2. The cellulose related activation energy increased in the SB. Due to briquetting, the lignin melted and spread in biomatrix to act as glue between the different particles. This writing considers that in addition to the lignin component, the hemicellulose also played important role during the briquetting. Hemicellulose and cellulose components thermally consolidated during briquetting process and took part in forming thermally stable briquette along with the lignin component.

4.3. Kissingger–Akahira–Sunose kinetics

The activation energy profiles with respect to α for SCR and SB were arrived by plotting the KAS kinetic lines. For arriving at this, the KAS points (1/T, $\ln(\beta/T^2)$) were extracted from the first order derivatives of thermogram (taken at all experimented β) at various selected conversion fraction. The plot of KAS lines, i.e., $\ln(\beta/T^2)$

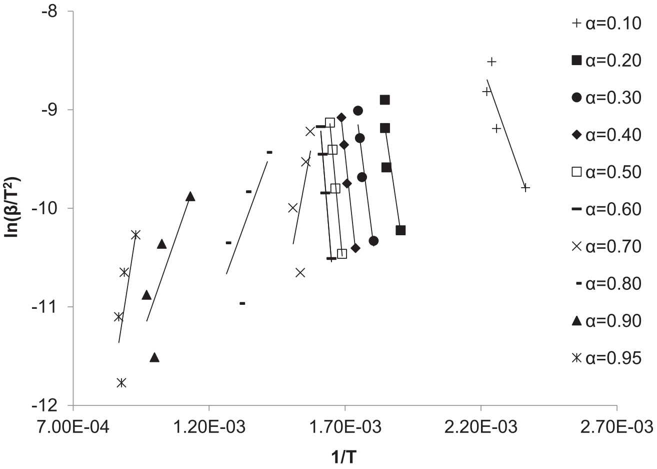

Fig. 9. KAS kinetic lines for SB at different isoconversional fraction.

Please cite this article in press as: Gangil S, Benefits of weakening in thermogravimetric signals of hemicellulose and lignin for producing briquettes from soybean crop residue, Energy (2015), http://dx.doi.org/10.1016/j.energy.2015.01.018

Table 3
KAS kinetics for SCR and SB (Linear correlation equations for KAS isoconversional lines ($\ln(\beta/T^2)$ *versus* 1/T)).

α	Soybean crop residue (SCR)			Briquette (SB)		
	Equation of linear fitting for KAS points	R^2		Equation of linear fitting for KAS points	R^2	
0	$y = 94,893x - 313.6$	0.68	×	$y = -45,369x + 137.68$	0.82	√
0.01	$y = -10,700x + 24.58$	0.85	√	$y = -25,459x + 67.462$	0.47	×
0.05	$y = -6768.2x + 10.001$	0.96	√	$y = -13,724x + 27.102$	0.80	√
0.10	$y = 3847.5x - 17.791$	0.49	×	$y = -7791.9x + 8.6167$	0.82	√
0.15	$y = -7706.3x + 5.2824$	0.06	×	$y = -14,082x + 18.141$	0.81	√
0.20	$y = -17,655x + 22.893$	0.19	×	$y = -18,490x + 24.968$	0.83	√
0.25	$y = -19,660x + 25.423$	0.32	×	$y = -19,885x + 26.432$	0.87	√
0.30	$y = -26,175x + 35.931$	0.53	×	$y = -21,462x + 28.359$	0.93	√
0.35	$y = -27,608x + 37.516$	0.62	×	$y = -23,447x + 31.08$	0.96	√
0.40	$y = -29,578x + 40.099$	0.66	×	$y = -25,360x + 33.663$	0.99	√
0.45	$y = -28,971x + 38.359$	0.63	×	$y = -27,963x + 37.414$	0.99	√
0.50	$y = -27,682x + 35.575$	0.49	×	$y = -29,930x + 40.077$	0.99	√
0.55	$y = -17,006x + 17.63$	0.16	×	$y = -31,708x + 42.432$	0.99	√
0.60	$y = 25,897x - 50.514$	0.60	×	$y = -33,504x + 44.749$	0.99	√
0.65	$y = 12,961x - 29.356$	0.92	√	$y = -48,194x + 67.414$	0.83	√
0.70	$y = 9720.1x - 23.703$	0.83	√	$y = 14,780x - 32.666$	0.43	×
0.75	$y = 8777.9x - 21.602$	0.64	×	$y = 8580x - 22.387$	0.53	×
0.80	$y = 6097x - 17.594$	0.36	×	$y = 7569x - 20.232$	0.51	×
0.85	$y = 715.34x - 11.372$	0.01	×	$y = 6974.6x - 18.72$	0.57	×
0.90	$y = -6076.8x - 5.0628$	0.23	×	$y = 7929.5x - 18.844$	0.63	×
0.95	$y = -8817.1x - 3.2663$	0.51	×	$y = 17,619x - 26.658$	0.56	×
0.99	$y = -11,586x - 1.4961$	0.60	×	$y = 71,139x - 68.989$	0.79	√
1.00	$y = 118,331x - 105.68$	0.95	√	$y = 107,492x - 96.932$	0.97	√

Where; $y = \ln(\beta/T^2)$ and $x = 1/T$.
The cut-off value of R^2 for performing further KAS analysis was 0.8.
× infers the KAS analysis inadequate for determination of kinetics.
√ infers the KAS analysis adequate for determination of kinetics.

versus 1/T at different α-values are given in Fig. 8 for SCR, and in Fig. 9 for SB. Table 3 shows equations of the linear KAS lines at different α-values for SCR and SB. During the TG-studies on plastic polymers and on specific biocomponents (like xylan, cellulose and lignin in extracted or separated or refined form), normally R^2 is taken as >0.9 for isoconversional kinetics. In case of biomaterials where one kind of biopolymeric molecules make complex linkages with other kind of molecules, the R^2 was taken as >0.8 considering the complexity in internal molecular networking during thermal degradation of biomaterials [4,5,30]. Activation energies for few α-points were not computed as shown in Table 3. The E-values obtained in present studies (Table 3) were in consonance with the E-values of lignocellulosic biomaterials as given by White et al. [26], Gangil [4,5,30,31,43,44] and Tsamba et al. [45]. Fig. 10 shows the dependency of activation energy on the conversion fraction for both biomaterials. The activation energies obtained from KAS and Kissinger method with respect of α is shown in Fig. 10. The approximate values of α were selected to plot the Kissinger E-points related to different biocomponent of both biomaterials. These approximate α-values were 0.05, 0.20, 0.50, 0.75, 0.90 for moisture, hemicellulose, cellulose, lignin and char, respectively, for SCR, and 0.55 for cellulose in case of SB. Activation energy profile of the SB was found superior than SCR.

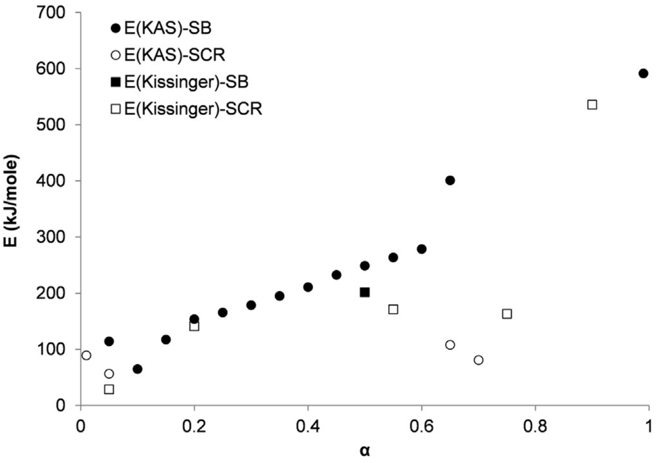

Fig. 10. Dependence of activation energy on conversional fraction.

5. Conclusions

Raw residues of soybean crop and its briquetted biofuel were analyzed and compared using thermogravimetric analysis. Kinetics was evaluated using the Kissinger and KAS methods. Thermogravimetric signals related to hemicellulose appeared to vanish due to briquetting. The activation energy profiles of raw residues of soybean crop and its briquetted form were compared to conclude that biomaterial of briquettes was thermally stable than the biomaterial of raw crop residues. The cellulose related activation energy levels were higher in briquettes. Low level of scattering of the tail end segment of thermogram in experimented domain of heating rates showed the lignin consolidation in briquette. Apart from the lignin, the hemicellulose and cellulose were also expected to play the positive role for briquetting.

Acknowledgments

The author is thankful to Director (CIAE); PC (AICRP on RES); Head (AEP); and CPI (NAIP-Biomass) for providing facilities and materials. Mr. P. K. Das, Mr. R. Powar, Mrs. S. S. Nevase, Ms. S. N. Mustapure, Mr. M. S. Verma, Mr. K. Kujur and Mr. R. H. Siddique are acknowledged for their help and support. The work presented in this article was accomplished as research activities under projects 489, 614, 656 and 670 of Central Institute of Agricultural Engineering, Bhopal, India.

Appendix A. Supplementary data

Supplementary data related to this article can be found at http://dx.doi.org/10.1016/j.energy.2015.01.018.

References

[1] Felfli FF, MesaP JM, Rocha JD, Filippetto D, Luengo CA, Pippo WA. Biomass briquetting and its perspectives in Brazil. Biomass Bioenergy 2011;35:236–42.
[2] Grover PD, Mishra SK. Biomass briquetting technology and practices. Food and Agriculture Organization (FAO); 1996. UN Document, No. 46, Available at: http://www.fao.org/docrep/006/ad579e/ad579e00.pdf.
[3] Singh RN, Vyas DK, Srivastava NSL, Narra M. SPRERI experience on holistic approach to utilize all parts of *Jatropha curcas* fruit for energy. Renew Energy 2008;33:1868–73.
[4] Gangil S. Beneficial transitions in thermogravimetric signals and activation energy levels due to briquetting of raw pigeon pea stalk. Fuel 2014;128:7–13.
[5] Gangil S. Polymeric consolidation in briquetted biofuel as compared to raw biomaterial: a TG-vision for pigeon pea stalks. Energy Fuels 2014;28:3248–54.
[6] Singh RN, Bhoi PR, Patel SR. Modification of commercial briquetting machine to produce 35 mm diameter briquettes suitable for gasification and combustion. Renew Energy 2007;32:474–9.
[7] Tripathi AK, Iyer PVR, Kandpal TC. A techno-economic evaluation of biomass briquetting in India. Biomass Bioenergy 1998;14:479–88.
[8] Singh J, Panesar BS, Sharma SK. Geographical distribution of agricultural residues and optimum sites of biomass based power plant in Bathinda, Punjab. Biomass Bioenergy 2011;35:4455–60.
[9] Tripathi AK, Iyer PVR, Kandpal TC, Singh KK. Assessment of availability and costs of some agricultural residues used as feedstocks for biomass gasification and briquetting in India. Energy Convers Manag 1998;39:1611–8.
[10] Tumuluru JS, Wright CT, Kenney KL, Hess JR. A technical review on biomass processing: densification, preprocessing, modeling and optimization. An ASABE Meeting Presentation Paper Number: 1009401, INL/CON-10–18636 PREPRINT, Available at: http://www.inl.gov/technicalpublications/documents/4559449.pdf.

[11] Purohit P, Tripathi AK, Kandpal TC. Energetics of coal substitution by briquettes of agricultural residues. Energy 2006;31:1321–31.
[12] Hu J, Lei T, Wang Z, Yan X, Shi X, Li Z, He X, Zhang Q. Economic, environmental and social assessment of briquette fuel from agricultural residues in China – a study on flat die briquetting using corn stalk. Energy 2014;64:557–66.
[13] Stolarski MJ, Szczukowski S, Tworkowski J, Krzyżaniak M, Gulczyński P, Mleczek M. Comparison of quality and production cost of briquettes made from agricultural and forest origin biomass. Renew Energy 2013;57:20–6.
[14] Abasaeed AE. Briquetting of carbonized cotton stalk. Energy 1992;17:877–82.
[15] Chen L, Xing L, Han L. Renewable energy from agro-residues in China: solid biofuels and biomass briquetting technology. Renew Sustain Energy Rev 2009;13:2689–95.
[16] Nasrin AB, Ma AN, Choo YM, Mohamad S, Rohaya MH, Azali A, Zainal Z. Oil palm biomass as potential substitution raw materials for commercial biomass briquettes production. Am J Appl Sci 2008;5:179–83. http://dx.doi.org/10.3844/ajassp.2008.179.183.
[17] Fengmin L, Mingquan Z. Technological parameters of biomass briquetting of macrophytes in Nansi Lake. Energy Procedia 2011;5:2449–54.
[18] Li Y, Li X, Shen F, Wang Z, Yang G, Lin L, Zhang Y, Zeng Y, Deng S. Responses of biomass briquetting and pelleting to water-involved pretreatments and subsequent enzymatic hydrolysis. Bioresour Technol 2014;151:54–62.
[19] Yumak H, Ucar T, Seyidbekiroglu N. Briquetting soda weed (*Salsola tragus*) to be used as a rural fuel source. Biomass Bioenergy 2010;34:630–6.
[20] Finell M, Nilsson C, Olsson R, Agnemo R, Svensson S. Briquetting of fractionated reed canary-grass for pulp production. Ind Crops Prod 2002;16:185–92.
[21] Vasile C, Popescu C, Popscu M, Brebu M, Willfor S. Thermal behavior/treatment of some vegetable residues. IV. Thermal decomposition of Eucalyptus wood. Cellul Chem Technol 2011;45:29–42.
[22] Caballero JA, Conesa JA, Front R, Marcilla A. Pyrolysis kinetics of almond shells and olive stones considering their organic fractions. J Anal Appl Pyrolysis 1997;42:159–75.
[23] López-González D, Fernandez-Lopez M, Valverde JL, Sanchez-Silva L. Thermogravimetric-mass spectrometric analysis on combustion of lignocellulosic biomass. Bioresour Technol 2013;143:562–74.
[24] Leadakowicz S, Stolarek P. Kinetics of biomass thermal decomposition. Chem Pap 2002;56:378–81.
[25] Sanchez-Silva L, López-González D, Villaseñor J, Sánchez P, Valverde JL. Thermogravimetric–mass spectrometric analysis of lignocellulosic and marine biomass pyrolysis. Bioresour Technol 2012;109:163–72.
[26] Damartzis T, Vamvuka D, Sfakiotakis S, Zabaniotou A. Thermal degradation studies and kinetic modeling of cardoon (*Cynara cardunculus*) pyrolysis using thermogravimetric analysis (TGA). Bioresour Technol 2011;102:6230–8.
[27] White JE, Catallo WJ, Legendre BL. Biomass pyrolysis kinetics: a comparative critical review with relevant agricultural residue case studies. J Anal Appl Pyrolysis 2011;91:1–33.
[28] Manikandan G, Jayabharathi J, Rajarajan G, Thanikachalam V. Kinetics and vaporization of anil in nitrogen atmosphere – non-isothermal condition. J King Saud Univ Sci 2012;24:265–70.
[29] Sbirrazzuoli N, Vincent L, Mija A, Guigo N. Integral, differential and advanced isoconversional methods complex mechanisms and isothermal predicted conversion–time curves. Chemom Intell Lab Syst 2009;96:219–26.
[30] Gangil S. Dominant thermogravimetric signatures of lignin in cashew shell as compared to cashew shell cake. Bioresour Technol 2014;155:15–20.
[31] Gangil S. Thermogravimetric evidence for better thermal stability in char produced under unconfined conditions. Environ Eng Sci 2014;31(4):183–92.
[32] Lu C, Song W, Lin W. Kinetics of biomass catalytic process. Biotechnol Adv 2009;27:583–7.
[33] Sait HH, Hussain A, Salema AA, Ani FN. Pyrolysis and combustion kinetics of date palm biomass using thermogravimetric analysis. Bioresour Technol 2012;118:382–9.
[34] Boyano A, Gálvez ME, Lázaro MJ, Moliner R. Characterization and kinetic study of carbon-based briquettes for the reduction of NO. Carbon 2006;44:2399–403.
[35] Chen W, Kuo P. Isothermal torrefaction kinetics of hemicellulose, cellulose, lignin and xylan using thermogravimetric analysis. Energy 2011;36:6451–60.
[36] Antal MJJ, Varhegyi G. Cellulose pyrolysis kinetics: the current state of knowledge. Ind Eng Chem Res 1995;34:703–17.
[37] Burhenne L, Messmer J, Aicher T, Laborie M. The effect of the biomass components lignin, cellulose and hemicellulose on TGA and fixed bed pyrolysis. J Anal Appl Pyrolysis 2013;101:177–84.
[38] Carrier C, Loppinet-Serani A, Denux D, Lasnier J, Ham-Pichavant F, Cansell F, Aymonier C. Thermogravimetric analysis as a new method to determine the lignocellulosic composition of biomass. Biomass Bioenergy 2011;35:298–307.
[39] Faravelli T, Frassoldati A, Migliavacca G, Ranzi E. Detailed kinetic modeling of the thermal degradation of lignins. Biomass Bioenergy 2010;34:290–301.
[40] Idris SS, Rahman NA, Ismail K, Alias AB, Rashid ZA, Aris MJ. Investigation on thermochemical behaviour of low rank Malaysian coal, oil palm biomass and their blends during pyrolysis via thermogravimetric analysis (TGA). Bioresour Technol 2010;101:4584–92.
[41] Abdullah SS, Yusup S, Ahmad MM, Ramili A, Ismail I. Thermogravimetry study on pyrolysis of various lingocellulosic biomass for potential hydrogen generation. Int J Chem Biol Eng 2010;3:137–41.
[42] Beyler CL, Hirschler. Chapter-7: thermal degradation of polymers. http://www.ewp.rpi.edu/hartford/~ernesto/F2012/EP/MaterialsforStudents/Patel/Beyler_Hirschler_SFPE_Handbook_3.pdf.
[43] Gangil S. Distinct splitting of cellulose related signals in cashew shell: a TG-diagnosis. Cellulose 2014;21:2913–24.
[44] Gangil S. Superiority of intrinsic biopolymeric constituents in briquettes of lignocellulosic crop residues over wood: a TG-diagnosis. Renew Energy 2015;76:478–83.
[45] Tsamba AJ, Yang W, Blasiak W. Pyrolysis characteristics and global kinetics of coconut and cashew nut shells. Fuel Process Technol 2006;87:523–30.

Please cite this article in press as: Gangil S, Benefits of weakening in thermogravimetric signals of hemicellulose and lignin for producing briquettes from soybean crop residue, Energy (2015), http://dx.doi.org/10.1016/j.energy.2015.01.018